

A Direct Interaction between the Utp6 Half- α -Tetratricopeptide Repeat Domain and a Specific Peptide in Utp21 Is Essential for Efficient Pre-rRNA Processing^{∇†}

Erica A. Champion,¹ Bennett H. Lane,² Meredith E. Jackrel,³ Lynne Regan,^{2,3} and Susan J. Baserga^{1,2,4*}

Departments of Genetics,¹ Molecular Biophysics and Biochemistry,² Chemistry,³ and Therapeutic Radiology,⁴
Yale University, New Haven, Connecticut 06520

Received 6 June 2008/Returned for modification 5 August 2008/Accepted 14 August 2008

The small subunit (SSU) processome is a ribosome biogenesis intermediate that assembles from its subcomplexes onto the pre-18S rRNA with yet unknown order and structure. Here, we investigate the architecture of the UtpB subcomplex of the SSU processome, focusing on the interaction between the half- α -tetratricopeptide repeat (HAT) domain of Utp6 and a specific peptide in Utp21. We present a comprehensive map of the interactions within the UtpB subcomplex and further show that the N-terminal domain of Utp6 interacts with Utp18 while the HAT domain interacts with Utp21. Using a panel of point and deletion mutants of Utp6, we show that an intact HAT domain is essential for efficient pre-rRNA processing and cell growth. Further investigation of the Utp6-Utp21 interaction using both genetic and biophysical methods shows that the HAT domain binds a specific peptide ligand in Utp21, the first example of a HAT domain peptide ligand, with a dissociation constant of 10 μ M.

In eukaryotes, ribosome biogenesis requires the coordinated processing and assembly of four ribosomal RNAs (rRNAs) and about 78 ribosomal proteins (49). In *Saccharomyces cerevisiae*, the 35S pre-rRNA is transcribed by RNA polymerase I in the nucleolus and is cleaved in several places to produce the mature 18S, 5.8S, and 25S rRNAs (Fig. 1). This process utilizes over 180 *trans*-acting factors and yet occurs fast enough to allow 2,000 ribosomes to be made each minute (for reviews, see references 16, 17, 22, 24, and 51). In this highly coordinated process, many factors assemble onto the nascent pre-rRNA as it is transcribed, forming large ribonucleoproteins (RNPs) that mature the small subunit (SSU) or large subunit (LSU) of the ribosome. Despite the identification of such *trans*-acting factors, the details of ribosome biogenesis remain elusive, as the complexity of ribosome biogenesis lies in the folding of pre-rRNAs and ribosomal proteins into functional ribosomes. Indeed, the frontier of ribosome synthesis investigation is to delineate the role(s) of each *trans*-acting factor in the production of the rRNA as it is modified, processed, and folded to become the mature ribosome (22).

Ribosome biogenesis is a dynamic process in which *trans*-acting factors associate with and dissociate from the evolving pre-rRNA throughout its maturation. The initial assembly of factors involved in both SSU and LSU biogenesis with the 35S pre-rRNA has been termed the 90S preribosome, which is separated by cleavage in ITS1 into the SSU processome (required for SSU maturation) and the 66S preribosome (required for LSU maturation) (22). An RNP forming around the

pre-18S rRNA has long been visualized in Miller chromatin spreads as a packed structure (35) in which the terminal knobs are thought to correspond to the SSU processome (37). The processome has been purified, and some of its components have been found in independent subcomplexes when the complete SSU processome has been pelleted and removed using high-speed ultracentrifugation (5, 13, 14, 21, 29, 40). As a first step to understanding the roles of various SSU processome proteins, several groups have undertaken the task of identifying the architecture of the subcomplexes and describing the order of their assembly into the SSU processome (19, 41). Yet much remains unknown about the pre-rRNA processing subcomplexes, notably, the order and manner by which the subcomplexes themselves assemble and how they assemble to form the preribosome.

To date, three subcomplexes have been identified as part of the SSU processome. The UtpA subcomplex is the first to assemble onto the pre-rRNA as it has been found to be associated with the rDNA and is required for its transcription (19). The UtpB subcomplex contains six proteins, each characterized by protein-protein interaction domains (Table 1): Utp1 (Pwp2), Utp12 (Dip2), Utp13, Utp18, and Utp21 contain WD40 repeats; Utp6 uniquely contains a half- α -TPR ([HAT] where TPR is tetratricopeptide repeat) domain (42), also referred to as a cl-TPR (crooked neck-like TPR) (9), crnTPR (crn-like TPR) (53), or RTPR (RNA-TPR) (4). Each of these proteins and their domains are conserved through eukaryotes, suggesting that the insight we gain by studying the assembly and function of this subcomplex in yeast is likely to extend to humans. Moreover, as genetic research in humans progresses, mutations in ribosomal proteins and ribosome biogenesis proteins are increasingly implicated in a variety of diseases. A testament to this relevance is the recent finding that a subset of neurofibromatosis patients bears a heterozygous deletion of *HCA66*, the human homolog of *UTP6* (28). Such a loss could lead to haploinsufficiency of the protein and inefficient ribo-

* Corresponding author. Mailing address: Department of Molecular Biophysics and Biochemistry, Yale School of Medicine, 333 Cedar Street P.O. Box 208040, C114 SHM, New Haven, CT 06520-8040. Phone: (203) 785-4618. Fax: (203) 785-6404. E-mail: susan.baserga@yale.edu.

† Supplemental material for this article may be found at <http://mcb.asm.org/>.

[∇] Published ahead of print on 25 August 2008.

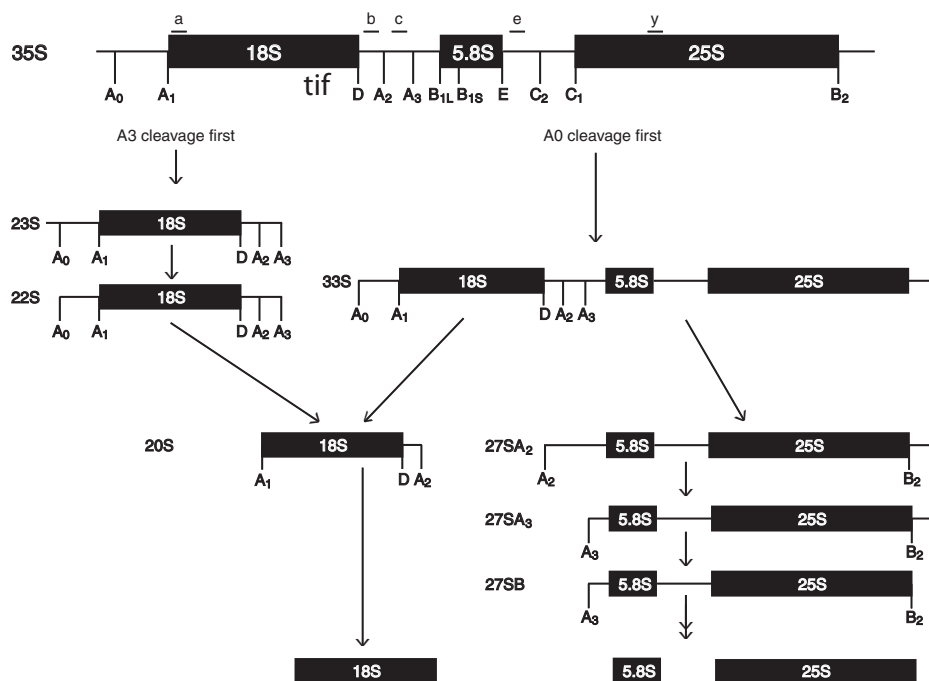


FIG. 1. Pre-rRNA processing in *S. cerevisiae*. The 35S primary transcript is cleaved in ITS1 to separate the pre-18S SSU rRNA from the pre-25S LSU rRNA. This may occur before (left) or after (right) cleavages A0, A1, and A2. If cleavage A3 occurs first, the resulting 23S rRNA is then cleaved at positions A0, A1, and A2 to produce the 20S pre-rRNA (left). If A0 cleavage occurs first, the resulting 33S pre-rRNA is then cleaved at A1 and A2, separating the 20S pre-rRNA from the 27SA2 pre-rRNA. In both schemes, the 20S pre-rRNA is exported from the nucleolus and cleaved at site D in the cytosol to produce the mature 18S rRNA, while the 27SA3/27SA2 undergoes further cleavages in the nucleolus to produce the mature 5.8S and 25S rRNAs, which are then exported to the cytosol. Locations of oligonucleotide probes used in northern analysis are shown (a, b, c, e, and y) (6).

some biogenesis, which may account for the increased disease severity these patients experience (12, 48).

In addition to its possible role in human disease, Utp6 is interesting because it contains the rare HAT motif, whose structure and function are only beginning to be understood. The HAT motif was discovered by its repeating pattern in the *Drosophila* crooked neck protein and was named by its sequence similarity to the TPR motif (53). In contrast to TPRs, the HAT motif is found only in proteins involved in RNA metabolism: in yeast Prp6, Prp39, Prp42, Clf1, and Syf1 participate in pre-mRNA splicing (4, 31, 34, 50); Utp6 and Rrp5 are required for pre-rRNA processing (14, 47); and Rna14 is involved in polyadenylation (3, 36). Each of these yeast proteins is essential, and each except Prp42 is conserved to hu-

mans. In addition to the conserved proteins listed above, there are two additional human HAT-containing proteins, SART3 and XAB2, both involved in pre-mRNA processing (1, 46). Each HAT-containing protein is thus a member of a protein complex involved in RNA metabolism, and in some cases the HAT-containing protein has been hypothesized to act as a keystone for other proteins in the complex or even as a link to RNA (Prp6 [31], Clf1 [50], and CstF-77 [3, 30]).

Such hypotheses about the function of the HAT domain are mostly based on the more extensive studies done on its cousin, the TPR domain (11). The TPR is a ubiquitous protein-protein interaction domain found in proteins with diverse functions. Several TPRs have been crystallized, and some have been cocrystallized with their ligands, which are typically peptides of 5 to 7 amino acids that bind in an extended conformation (7, 45). In contrast, though a structure of the CstF-77 HAT domain was solved (3, 30), little is known about the function of the HAT domain in RNP assembly. Several proteins have been found to interact with HAT-containing proteins using both two-hybrid and in vitro pull-downs, but no specific ligand for a HAT domain has been identified (3, 4, 31, 50).

In this study, we have sought to delineate the function of the HAT domain in Utp6 and its role in the assembly of the UtpB subcomplex of the SSU processome. We have analyzed the effects of point mutations and deletion mutations in the Utp6 HAT domain on pre-rRNA processing and cell growth and found that the HAT domain is essential for both. We have also used a yeast two-hybrid approach to determine the overall architecture of the

TABLE 1. Proteins in the SSU processome UtpB subcomplex^a

Yeast protein (mass [kDa])	Accession no. of human homolog (mass [kDa])	Conserved structural element(s)
Utp1/Pwp2 (103.9)	NP_005040.2 (102.5)	WD40, Pwp2 domain
Utp6 (52.3)	NP_060898.2 (70.2)	HAT
Utp12/Dip2 (106.3)	NP_006775.1 (106.3)	WD40, Dip2 domain
Utp13 (91.0)	NP_006444.2 (91.2)	WD40, Utp13 domain
Utp18 (66.4)	NP_057085.2 (62.0)	WD40
Utp21 (104.8)	NP_644810.1 (105.3)	WD40, Utp21 domain

^a The UtpB subcomplex of the SSU processome in yeast consists of six proteins, each of which has a human homolog (based on sequence similarity). Structural elements found in the yeast proteins are conserved in the human homologs.

```

TPR      ...Y...A...Y...A...P...W...G...Y...
HAT      ...RAR...YER...W...YA...FE...
Utp6 HAT1 WSTQORIGFIQRGTNKRFPQDLLKFAAMLNLMYKAR (86-119)
Utp6 HAT2 QTSYKKIHNINQLLLLKTHPTNVDIIISCAKYEYE (123-156)
Utp6 HAT3 HANFKSCRNIFQNGLRFNPDVPKLYEVYKFELN (158-191)

```

FIG. 2. Utp6 contains three HAT repeats. The TPR consensus (33) is aligned with the HAT consensus and the three HAT repeats in Utp6. Boxes surround residues in Utp6 that are predicted to form alpha helices based on the TPR structure (11). Note that in TPRs, the conserved W is at position 4, and the conserved P is at position 32, resulting in a repeat that encodes helix A followed by helix B. In HATs, helix B is followed by helix A; this alignment reflects the HAT consensus. Dark shading indicates residues in Utp6 that are identical to the HAT consensus sequence; light shading indicates residues in Utp6 that are similar to the HAT consensus.

UtpB subcomplex, as well as to identify a peptide ligand within Utp21 for the Utp6 HAT domain, an interaction that has been confirmed by our biophysical approach. We propose that the mutations we have created in the HAT domain abrogate binding to Utp21 and that the disruption of this interaction causes a barrier to SSU processome assembly.

MATERIALS AND METHODS

Bioinformatics and genetic screen for cold sensitivity. The HAT consensus sequence was determined using an alignment of 745 HAT sequences downloaded from the SMART database (<http://smart.embl-heidelberg.de/>) and identifying amino acids that are conserved in at least 40% of the sequences at a given position (Fig. 2).

To generate random point mutations in *UTP6* for the genetic screen, *UTP6* was amplified using disproportionate amounts of deoxynucleoside triphosphates (at a ratio of 5:1 for CT to GA or GA to CT) and primers that add restriction sites and 50 nucleotides homologous to the p415GPD vector (39) to each end of the PCR product to facilitate gap repair (38). The PCR product was cotransformed with the cut p415GPD vector into YPH499 (*MATa ura3-52 lys2-801 ade2-101 trp1-Δ63 his3-Δ200 leu2-Δ1 GAL::3HA-UTP6* (which includes three copies of a hemagglutinin tag [HA]) and plated on medium with glucose and lacking leucine. Colonies were restreaked onto new plates and then replica plated to test for growth at 17°C and 30°C. Plasmids were extracted from cold-sensitive colonies by Hirt lysis, passed through *Escherichia coli* DH5α, and retransformed into yeast to test for plasmid dependence of the cold sensitivity. Plasmids carrying *utp6* that conferred a cold-sensitive growth defect were sequenced; all sequencing described was performed by the W. M. Keck Foundation facility at the Yale School of Medicine (see Table S1 in the supplemental material).

Site-directed mutagenesis was performed on wild-type *UTP6* cloned into p415GPD using a Stratagene QuikChange Kit and mutagenic oligonucleotides (see Table S3 in the supplemental material). All inserts were fully sequenced (see Table S2 in the supplemental material).

Growth assays and Western blotting. YPH499 *GAL::3HA-UTP6* containing the appropriate *utp6* gene in p415GPD was grown to stationary phase in synthetic medium lacking leucine and containing 2% galactose and 2% raffinose. For serial dilutions, 0.2 ml of cells at an optical density at 600 nm (OD_{600}) of 1 was resuspended in 1 ml of water, and 1/10 serial dilutions were plated on medium with glucose and lacking leucine. Cells were grown at 21°C, 30°C, or 37°C for 3 days or at 17°C for 6 days.

For Western blotting, starter cultures were depleted of endogenous Utp6 by growth in glucose medium lacking leucine for 24 h at 21°C, 30°C, or 37°C. For each culture, 10 ml of cells at an OD_{600} of ~0.5 was collected, washed with water, resuspended in 200 μl of NET-2 (20 mM Tris-Cl, pH 7.5, 150 mM NaCl, 0.05% Nonidet P-40) with protease inhibitors (Roche mix), and lysed with 0.45- to 0.5-mm glass beads. The lysate was cleared by centrifugation for 10 min at 13,200 rpm at 4°C. Total protein (15 μl) was separated by 10% sodium dodecyl sulfate-polyacrylamide gel electrophoresis (SDS-PAGE) and transferred onto a nitrocellulose membrane. Utp6 expression was tested by Western blot analysis using an antihemagglutinin (anti-HA) antibody (12CA5 at 1:200 dilution in culture supernatant). Mpp10 expression was tested by Western blot analysis using an anti-Mpp10 antibody (15).

Northern analysis. Cells were grown as described for Western blot analysis, and then RNA was extracted from 10 to 20 ml of cells at an OD_{600} of ~0.5 using

the acid phenol method (2). Twenty micrograms of RNA was run on a 1.25% formaldehyde-agarose gel, transferred to Amersham Hybond-N+ membrane, and probed as described previously (6).

Coimmunoprecipitations. Cells were grown and lysed as described for Western blot analysis except that 20 ml of cells at an OD_{600} of ~0.5 was lysed in 600 μl of NET-2. Anti-HA antibody (400 μl per sample) was coupled to 5 mg of protein A-Sepharose CL-4B beads by incubation overnight at 4°C on a nutator. Beads were washed three times with 1 ml of NET-2 and then incubated with cell lysate for 1 h at 4°C. Beads were then washed five times with 0.5 ml of NET-2 to clear unbound protein and then resuspended in 10 μl of SDS loading dye. Both total protein (5%) and immunoprecipitates were separated by 10% SDS-PAGE and transferred onto a nitrocellulose membrane. Western blot analysis of immunoprecipitates used the previously mentioned anti-Mpp10 antibody.

Yeast two-hybrid analysis. Genes encoding UtpB subcomplex members (Utp1, Utp6, Utp12, Utp13, Utp18, and Utp21) and deletion mutants of Utp6 were cloned into the pAS2-1 (bait, *TRP1* marker) and pACT2 (prey, *LEU2* marker) vectors using PCR primers (see Table S3 in the supplemental material). *utp6* constructs containing point mutations were subcloned from p415GPD. Deletion mutants of Utp21 were constructed by QuikChange (Stratagene) mutagenesis of a given codon to a stop codon (for residues 1 to 938, 1 to 689, 1 to 327, and 1 to 207), by PCR using the oligonucleotides listed in Table S3 in the supplemental material (for residues 1 to 273, 1 to 279, 1 to 283, and 1 to 299), or for fragment 1 to 242 by digestion at a serendipitous BamHI site, which allows the encoding from the vector of nine additional amino acids following residue 242 (IRAREI YE). All inserts were fully sequenced.

Vectors were transformed sequentially into the yeast strain pJ69-4a (27), which contains *HIS3* under a *GAL4* promoter. Cells were serially diluted as described above but using 0.4 ml of cells at an OD_{600} of 1 or struck out on double selection medium (lacking leucine and tryptophan) to select for both vectors or triple selection medium (lacking leucine, tryptophan, and histidine) to assess whether a given pair of proteins interact.

Recombinant protein preparation. The *UTP6* gene (wild-type or containing the G99E mutation) was cloned into a derivative of the maltose binding protein (MBP) fusion vector pMAL-c2x (New England Biolabs) containing a target site for the tobacco etch virus protease in place of the Factor X protease site (43). MBP, MBP-Utp6-6HIS, and MBP-Utp6-G99E-6HIS were expressed as recombinant proteins in *E. coli* BL21(DE3) cells using standard methods. Purifications were either single step (amylose resin; New England Biolabs) or two step (amylose resin followed by nickel charged resin, Ni²⁺-nitriloacetic acid agarose; Qiagen Inc.).

Surface plasmon resonance binding (SPR) assays. The Utp21 peptide ligand (biotin-GGG-GTSSGDLIFYDLDL-CONH2) was synthesized by the W. M. Keck Foundation (Yale School of Medicine). A biotin moiety and a three-glycine residue spacer were appended at the N terminus as indicated above. The C terminus was amidated to better mimic an internal peptide.

SPR analysis was carried out using a CM5 sensor chip in a Biacore 3000 system (Biacore). The chip was derivatized using standard amine-coupling chemistry to immobilize NeutrAvidin (Pierce), yielding a final response unit total of 2,880. Biotinylated peptide was dissolved in HBS-EP (150 mM NaCl, 5 mM EDTA, 0.005% [vol/vol] polysorbate 20, 10 mM HEPES, treated to pH 7.4) buffer, and this solution was injected over one channel, resulting in an increase of 220 response units, corresponding to NeutrAvidin-bound peptide. A separate channel to be used for background correction was similarly prepared with immobilized NeutrAvidin but without injection of biotinylated peptide. Excess free biotin was injected in both channels to block any unbound NeutrAvidin sites.

Binding experiments were carried out using solutions of proteins prepared in buffer T (25 mM Tris-HCl, 150 mM NaCl, 0.01% Igepal, 1 mM EDTA, pH 7.4 at 25°C). Protein (200 μl) was injected in the Kinject mode (40 μl/min flow rate), followed by a 250-s dissociation period. Between injections, the chip surface was regenerated by two 40-μl injections of 1 M NaCl. In all cases, injections occurred in both the peptide-bound and background channels.

A steady-state one-site binding model was used for curve-fitting of average response values at steady-state equilibrium versus concentration according to the following equation: $R_{eq} = R_{max}[P]/(K_d + [P])$, where R_{eq} is the average response value at steady-state equilibrium, R_{max} is the response value at saturation, $[P]$ is the protein concentration, and K_d is the dissociation constant. Curve fitting reported the value of the dissociation constant.

RESULTS

Derivation of mutations in Utp6. We hypothesized that the HAT domain of Utp6 participates in a protein-protein inter-

action that is essential for the assembly of the SSU processome. Further, we expected that if we could identify mutations that disrupt only the HAT-mediated protein-protein interaction, we could identify the peptide ligand for the HAT domain. This would lend insight to the structure and function of HAT domains, for which no ligand had yet been found. Because Utp6 is essential and because we aimed to disrupt only the function of the HAT domain, we used random and directed mutagenesis to generate a pool of mutations in the HAT domain of Utp6 with the potential of disrupting HAT function and ribosome assembly.

Previously, a genome-wide screen for cold sensitivity in bacteria found a high proportion of genes involved in ribosome assembly, illustrating that cold-sensitive mutations are a hallmark of defects in macromolecular assembly (23). Based on this study and our aim to identify mutations that cause defects in ribosome assembly rather than mutations that disrupt protein folding (typically temperature sensitive [20]), we searched for mutations in Utp6 that confer cold sensitivity.

First, we created a library of randomly mutagenized *UTP6* (38) genes. Colonies expressing randomly mutated Utp6 proteins were tested for growth at different temperatures. Colonies that grew the same as wild type at 30°C but not at 17°C were identified as cold sensitive. Though the screen was not exhaustive, we identified 13 cold-sensitive strains containing a mutated Utp6, most of which contained several mutations (see Table S1 in the supplemental material). Four strains included mutations that encode a premature stop (stops at positions Q211 and Q219 and frameshifts at positions 232 and 238), producing in each case a Utp6 protein that is truncated by about half, just C-terminal to the HAT3 motif. Remarkably, these truncated Utp6 proteins were sufficient to support growth at 30°C. The remaining nine strains contained mutated Utp6 proteins with several amino acid changes, some of which were tested further to determine which were singularly causing the cold-sensitive phenotype. Of these mutations (see Table S1 in the supplemental material), two were chosen for further study. Q219Z is the only mutation found in strain cs-16, which causes a truncation of 28 amino acids C-terminal to the HAT3 motif. G99E, in cs-2, is found in a conserved, small aliphatic position of the HAT1 motif and confers a strong cold-sensitive phenotype.

Our second approach to identify mutations in Utp6 used bioinformatics to predict which amino acid residues in the HAT domain might, when mutated, confer a cold-sensitive growth defect. Residues conserved among HAT proteins are likely to be involved in the structure of the HAT domain, and residues conserved among only Utp6 homologs are likely to be involved in the particular function of the Utp6 protein (Fig. 2) (32). Representative amino acids were mutated and tested for cold sensitivity (see Table S2 in the supplemental material). Three of these mutations were chosen for further study. L114D is found in an aliphatic position of the HAT1 motif and confers a strong cold-sensitive phenotype. W147A is found in the most highly conserved position 4 of the HAT2 motif and confers a weak cold-sensitive phenotype. A third mutation, K180Z, was created to test a gross disruption of the HAT domain. This mutation truncates Utp6 within the HAT3 motif, eliminating the final predicted alpha helix, and does not complement Utp6 depletion at any temperature tested.

Mutations in the HAT domain of Utp6 confer growth defects. Strains carrying each of the five mutations in Utp6 (K180Z, Q219Z, G99E, L114D, and W147A) were further tested for growth defects. In these strains the endogenous *UTP6* was placed under a galactose-inducible, glucose-repressible promoter. The mutated *utp6* genes were expressed from a plasmid using a constitutive promoter. To ensure that the mutated Utp6 proteins were being expressed, we used 3HA tags and Western blotting to identify the mutated proteins after 24 h of growth in glucose (Fig. 3A). The levels of endogenous Utp6 were greatly reduced after 3 h of growth in glucose (data not shown). Each mutated protein was expressed at comparable levels, with the exception of Utp6 carrying a G99E mutation (Utp6-G99E), which was expressed at lower levels when cells were grown at higher temperatures (30°C and 37°C). As is the case with temperature-sensitive mutations in general (20), this is likely to be caused by misfolding of the protein, followed by degradation at higher temperatures.

We assayed for temperature-dependent growth defects using growth on solid medium with glucose (Fig. 3B). Compared to the wild type, each of the mutations conferred growth defects to various extents at nonpermissive temperatures. Utp6-K180Z was unable to support growth at any temperature. Another strong defect was observed in the strain carrying Utp6-G99E, at least in part due to the reduced protein levels observed in Fig. 3A. At lower temperatures (21°C and 17°C), however, when Utp6-G99E was stably expressed, a defect was still observed. The three other mutations (Q219Z, L114D, and W147A) also conferred temperature sensitivity and cold sensitivity, with the weakest cold-sensitive phenotype in the strain carrying Utp6-W147A. These phenotypes are likely due to a defect in macromolecular assembly, based on the previous findings in *E. coli* that assembly-defective mutants of ribosome biogenesis proteins confer a cold-sensitive phenotype (23).

Mutations in the HAT domain of Utp6 confer defects in pre-rRNA processing. While the cold-sensitive phenotype of mutations in Utp6 implies that these mutations render steps in ribosome assembly less efficient, it is possible that the HAT domain of Utp6 has an alternate essential role separate from ribosome biogenesis. To determine whether the mutations in the HAT domain cause a defect in ribosome biogenesis, we examined steady-state levels of pre-rRNA species in strains expressing only mutated Utp6 proteins. Total RNA was probed using Northern blotting with radiolabeled oligonucleotides specific to pre-rRNA sequences (Fig. 1 and 4).

Depletion of Utp6 (Fig. 4, vector lanes 2, 9, and 16 in glucose panels) resulted in a decrease in the 27SA2 and 20S pre-rRNAs and in the mature 18S rRNA. We also observed an accumulation of the 23S pre-rRNA. This is typical for depletion of an SSU processome protein, which causes defects at cleavages A0, A1, and A2 (Fig. 1) (19). Deletion mutants Utp6-K180Z and Utp6-Q219Z mimic the Utp6 depletion at all three temperatures (Fig. 4, lanes 3, 4, 10, 11, 17, and 18 in glucose panels), suggesting that these are reduced in cleavage at all three sites. This finding is surprising because we previously found that Utp6-Q219Z confers minimal growth defects at 30°C. As expected, the point mutations confer intermediate defects, with the strongest pre-rRNA processing defects corresponding to the strongest growth defects (Fig. 4, lanes 5, 6, 7, 12, 13, 14, 19, 20, and 21 in glucose panels). The LSU 27SB

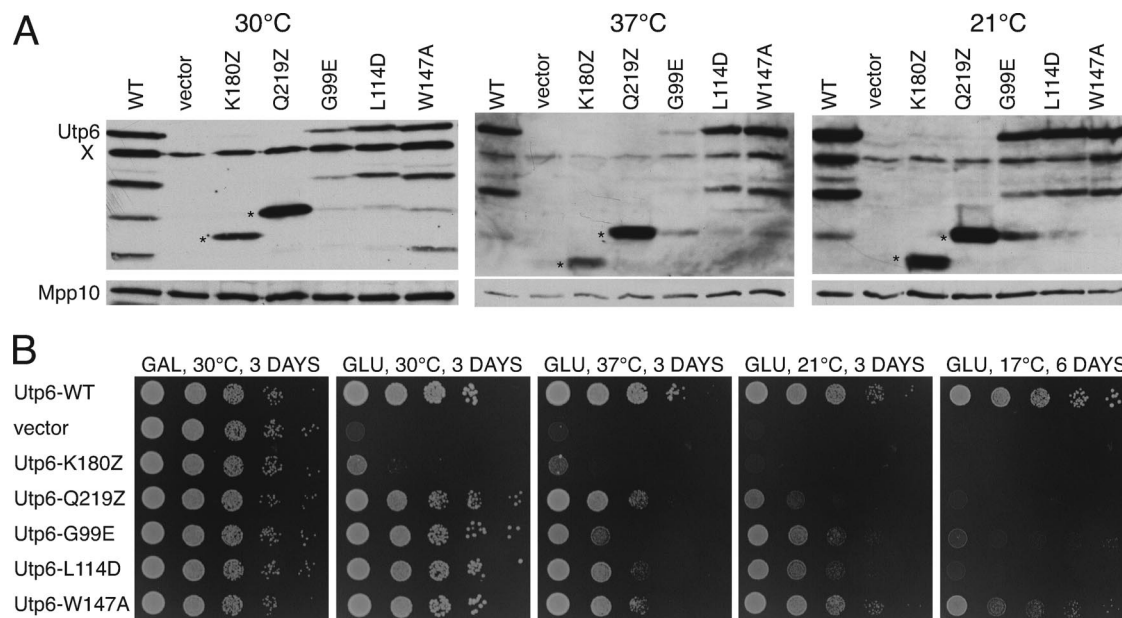


FIG. 3. Mutations in Utp6 confer growth defects. (A) Yeast expressing wild-type Utp6 (WT), no Utp6 (vector), or a mutated Utp6 (K180Z, Q219Z, G99E, L114D, or W147A) was grown for 24 h in medium containing glucose at 30°C, 37°C, or 21°C. Utp6 expression was assayed by Western blotting with anti-HA antibody. Truncation mutant bands are marked by an asterisk. A cross-reacting band, present in all lanes, is marked by X. Western blotting for Mpp10 was used as a loading control. (B) Yeast expressing wild-type Utp6 (WT), no Utp6 (vector), or a mutated Utp6 (K180Z, Q219Z, G99E, L114D, or W147A) was serially diluted and spotted onto medium containing galactose (GAL) and grown at 30°C or onto medium containing glucose (GLU) and grown at 30°C, 37°C, 21°C, or 17°C.

pre-rRNA and 25S rRNA were not affected by mutations in Utp6. Interestingly, neither 21S nor 22S pre-rRNAs accumulated in Northern analysis of Utp6 point mutants (Fig. 4, lanes 5, 6, 7, 12, 13, 14, 19, 20, and 21 in glucose panels), as previously observed with mutations in other SSU processome proteins, Imp4, Mpp10, and Utp24 (6, 18, 52). This suggests that even single point mutations in Utp6 affect processing at all three sites, A0, A1, and A2. Taken together, these data indicate that mutations in the HAT domain of Utp6 have a specific effect on pre-rRNA processing.

The effect of mutations in the HAT domain of Utp6 on its association with the SSU processome. Our hypothesis is that the HAT domain in Utp6 mediates a protein-protein interaction required for assembly of the SSU processome. Thus far, we have shown that mutations in the HAT domain cause defects in pre-rRNA processing with concomitant growth defects. We therefore reasoned that the mutations in the HAT domain of Utp6 are causing these defects by preventing the HAT-mediated protein-protein interaction. Specifically, we expected that the K180Z, Q219Z, and G99E mutations, which exhibit the strongest growth and pre-rRNA processing defects, would also exhibit a lesser ability to associate with the SSU processome. To test this, we performed immunoprecipitations of 3HA-tagged, mutated Utp6 and investigated whether Mpp10, another SSU processome protein used as a marker for the complete SSU processome, would coprecipitate (Fig. 5).

Unexpectedly, none of the mutations in Utp6 had a deleterious effect on its ability to associate with Mpp10 in the immunoprecipitations (Fig. 5, IP lanes). Only the strain containing Utp6-G99E grown at 37°C, which was previously shown to be expressed at very low levels (Fig. 3A), did not considerably

associate with Mpp10. Other point mutants, Utp6-L114D and Utp6-W147A, were found to associate with Mpp10 at all temperatures tested, though perhaps to a lesser extent than the wild type. Deletion mutants Utp6-K180Z and Utp6-Q219Z, which confer severe growth defects (Fig. 3B) and pre-rRNA processing defects (Fig. 4) immunoprecipitate slightly reduced amounts of Mpp10 at all temperatures. This suggests that the pre-rRNA processing defect observed due to mutations in the HAT domain of Utp6 is not caused by a simple inability of the protein to associate with the SSU processome in the steady-state.

Subunit architecture of the UtpB subcomplex. Because no identified HAT domain has yet been linked to a specific ligand, we set out to identify a ligand for the HAT domain in Utp6. If the HAT domain is indeed a protein-protein interaction motif, it is likely that the HAT domain in Utp6 mediates an interaction with one of the other five UtpB subcomplex proteins. We therefore started by using a directed yeast two-hybrid approach to evaluate pairwise interactions between proteins in the UtpB subcomplex.

Each UtpB subcomplex protein (Utp1, Utp6, Utp12, Utp13, Utp18, and Utp21) was cloned into each two-hybrid vector, bait and prey, and expressed in the two-hybrid host strain, pJ69-4a, which contains the *HIS3* gene under a *GAL4* promoter, so that interaction between bait and prey fusion proteins could be determined by growth on medium lacking histidine. Cells were spotted onto permissive or selective medium, and interactions were evaluated (Fig. 6A).

The results indicate that Utp21 and Utp18 interact with each other and that each interacts with Utp6 and Utp1. Utp13 interacts only with Utp12, which also interacts with Utp21. The

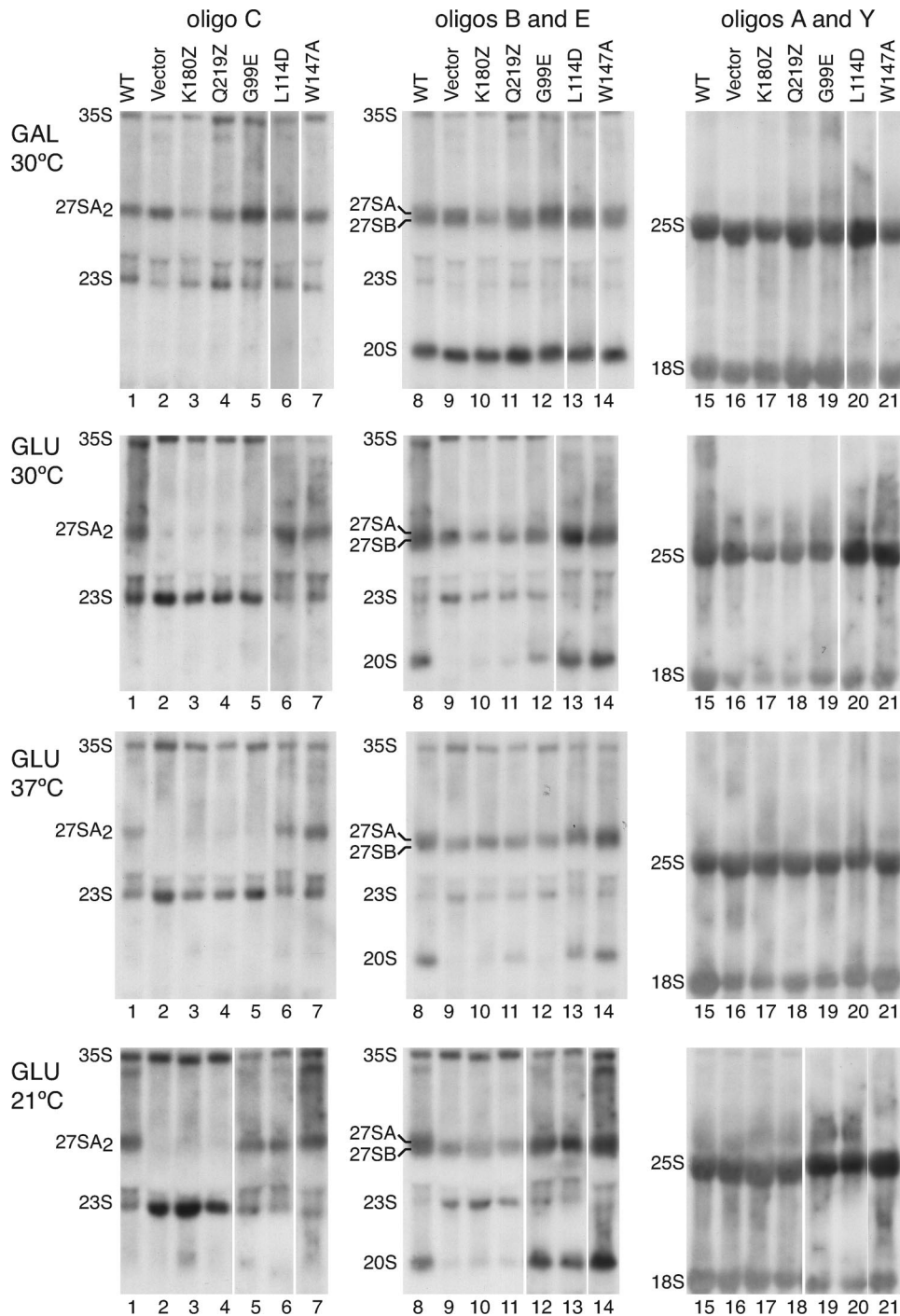


FIG. 4. Mutations in Utp6 confer defects in pre-rRNA processing. Yeast expressing wild-type Utp6 (WT), no Utp6 (vector), or a mutated Utp6 (K180Z, Q219Z, G99E, L114D, or W147A) was shifted from medium containing galactose (GAL) at 30°C to medium containing glucose (GLU) and grown for 24 h at 30°C, 37°C, or 21°C. Total RNA was extracted, and equal amounts of RNA were separated on an agarose-formaldehyde gel, then transferred to a Hybond-N+ membrane, and probed using radiolabeled oligonucleotides (oligos) that hybridize to pre-rRNA as shown in Fig. 1.

network of the protein-protein interactions is depicted in Fig. 6D. The Utp18-bait fusion protein activated transcription of the *HIS3* reporter even in the presence of a null-prey fusion (empty prey vector), so we were unable to assess interactions with Utp18 as the bait. Interestingly, Utp6 is the only protein found to interact with itself.

The HAT domain of Utp6 is necessary for interaction with Utp21 but not Utp18. Because Utp6 interacts with both Utp21 and Utp18 in the two-hybrid system, we tested whether either of these proteins binds to Utp6 via the HAT domain using deletion mutants of Utp6 in the two-hybrid system (Fig. 6B). The Utp6 protein sequence can be divided into three domains:

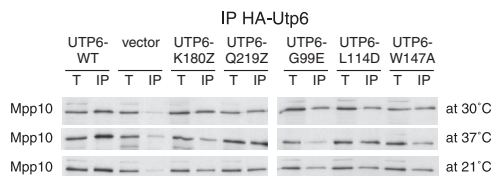


FIG. 5. Mutations in Utp6 do not disrupt association with the SSU processome. Yeast expressing wild-type Utp6 (WT), no Utp6 (vector), or a mutated Utp6 (K180Z, Q219Z, G99E, L114D, or W147A) was grown in medium containing galactose at 30°C, then shifted to medium containing glucose, and grown for 24 h at 30°C, 37°C, or 21°C. Total protein was extracted and 3HA-tagged Utp6 was immunoprecipitated. The immunoprecipitate (IP) and 5% of the total protein (T) extract were separated by SDS-PAGE and transferred to a nitrocellulose membrane. The presence of Mpp10, a marker for the SSU processome, was assayed by Western blotting.

the N terminus (amino acids 1 to 84), the HAT domain (84 to 194), and the C terminus (194 to 440). We cloned several combinations of these domains into the two-hybrid bait vector and tested them for interaction with Utp18 and Utp21. Both

Utp18 and Utp21 interact with full-length Utp6 and Utp6 truncated at Q219. Utp21 does not interact with Utp6 truncated at K180, in which the HAT domain is disrupted. In contrast, Utp18 interacts with both the Utp6 K180 truncation and with the Utp6 N terminus alone, indicating that the HAT domain is not essential for interaction with Utp18 but that an intact HAT domain is necessary for interaction with Utp21. As expected, an empty prey vector shows no interaction with any Utp6 bait.

We hypothesized that a mutation in the HAT domain would disrupt a protein-protein interaction, thereby inhibiting pre-rRNA processing. We earlier identified three point mutations in the HAT domain that confer defects in pre-rRNA processing and could potentially disrupt a protein-protein interaction. To test this hypothesis, we created the point mutations (G99E, L114D, and W147A) in Utp6 in the two-hybrid bait vector and tested the mutated Utp6 for interaction with both Utp18 and Utp21 (Fig. 6C). While the weaker mutations L114D and W147A did not disrupt the interaction of Utp6 with either Utp18 or Utp21, the G99E mutation disrupted the interaction

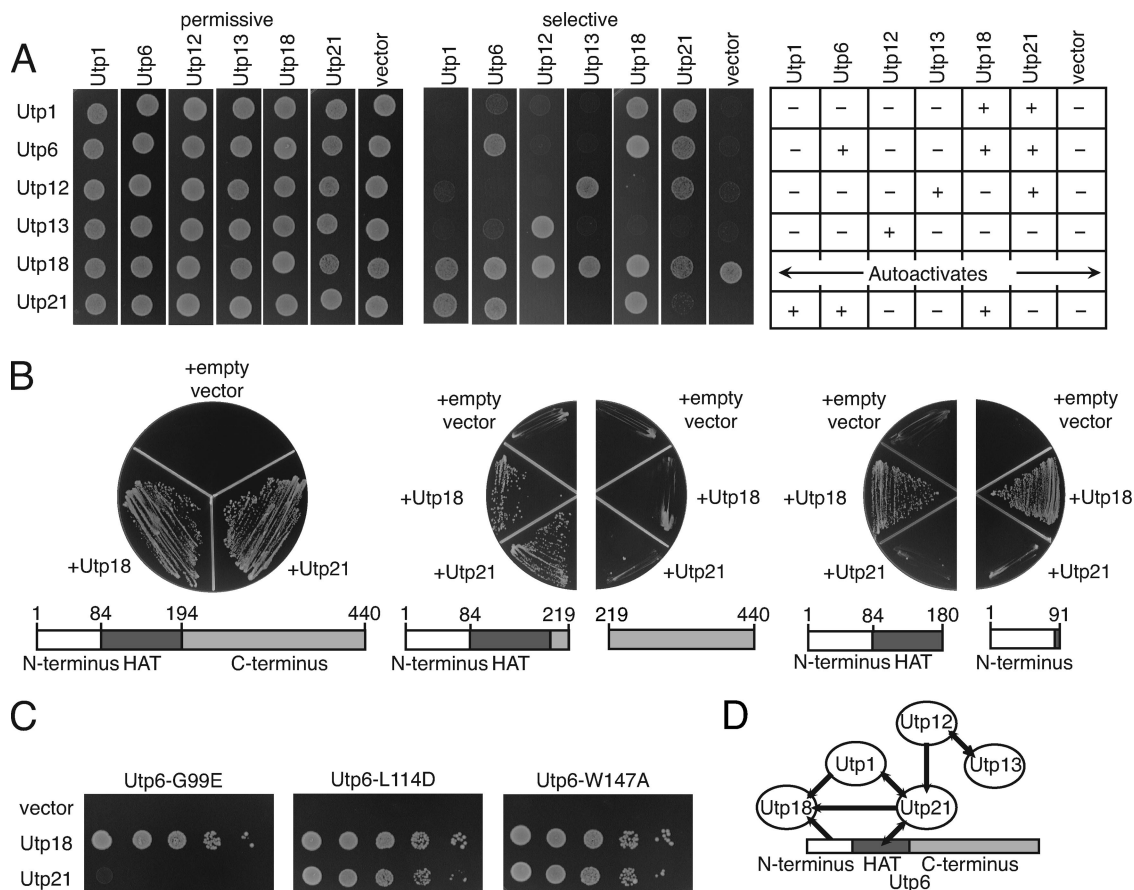


FIG. 6. Subunit architecture of the UtpB subcomplex. (A) Yeast was transformed with a given bait (left) and a given prey (top) and tested for its ability to grow on medium containing histidine (permissive) or lacking histidine (selective). Positive protein-protein interactions are indicated by growth on selective medium. +, positive interaction; -, negative interaction. (B) Yeast was transformed with a vector encoding a Utp6-bait fusion using wild-type Utp6 or Utp6 deletion mutants, diagrammed as shown below the plates, and with a prey vector with no insert (+empty vector), a Utp18-prey fusion (+Utp18), or a Utp21-prey fusion (+Utp21). Protein-protein interaction was tested by growth on medium lacking histidine. (C) Yeast was transformed with a vector encoding a Utp6 mutant-bait fusion as shown and with a prey vector with no insert (vector), a Utp18-prey fusion (Utp18), or a Utp21-prey fusion (Utp21), and protein-protein interaction was tested by growth on medium lacking histidine. (D) Positive interactions from panels A to C are summarized. Arrows point from bait to prey.

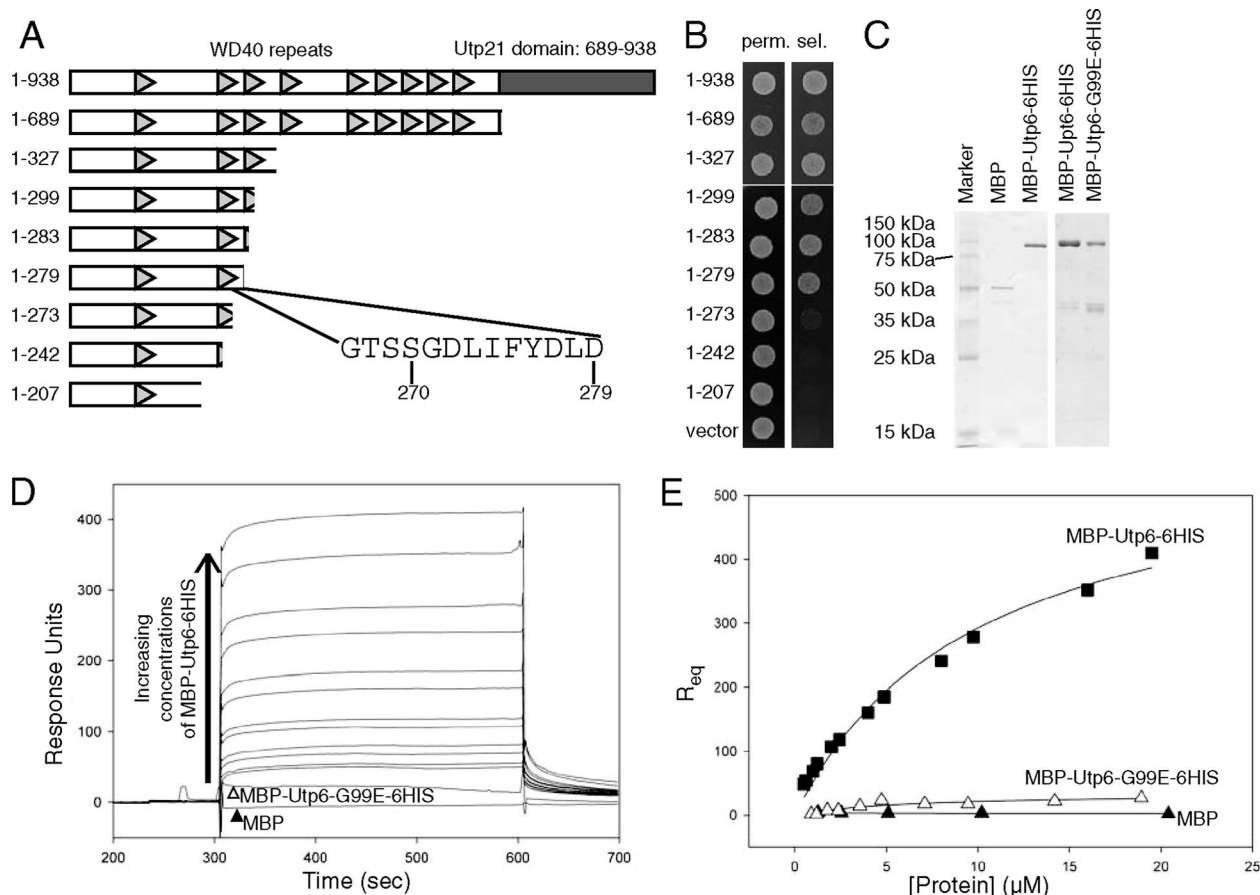


FIG. 7. Utp6 binds to a specific short peptide in Utp21. (A) Schematic of domain organization in wild-type Utp21 and Utp21 truncation mutants. Arrowheads and a shaded box represent WD40 repeats and the Utp21 domain, respectively. The sequence and location of the Utp21 peptide ligand are illustrated. (B) Two-hybrid analysis of Utp21 truncation mutants. Yeast containing Utp6 in bait vector and the indicated Utp21 truncation in prey vector was spotted onto medium containing (permissive [perm]) or lacking (selective [sel]) histidine and tested for growth. (C) MBP prepared by amylose affinity purification and MBP-Utp6-6HIS prepared by purification with both amylose and nickel affinity steps were analyzed by SDS-PAGE (left). MBP-Utp6-6HIS and MBP-Utp6-G99E-6HIS were analyzed by SDS-PAGE; both were prepared by amylose affinity purification (right). (D) Sensorgrams showing protein interactions with the Utp21 peptide. MBP-Utp6-6HIS was tested in increasing concentrations; from bottom to top, as indicated by the arrow, these concentrations were 0.50, 0.61, 1.00, 1.22, 2, 2.44, 4, 4.88, 8, 9.75, 16, and 19.5 μ M. The sensorgrams of MBP-Utp6-G99E-6HIS at a concentration of 18.9 μ M (open arrowhead) and MBP at 91.2 μ M (filled arrowhead) are indicated. All sensorgrams were corrected for nonspecific binding. (E) Dependence of average equilibrium response (R_{eq}) on protein concentration. MBP (filled triangles) or MBP-Utp6-G99E-6HIS (open triangles) does not show significant interaction; the dissociation constant calculated by fitting the data from MBP-Utp6-6HIS (filled squares) to a steady-state one-site binding model is 10 μ M.

with Utp21 but not with Utp18. This was confirmed using the mutated Utp6 as the prey and Utp21 as the bait (data not shown). These findings support the hypothesis that Utp21 interacts with Utp6 via its HAT domain.

Identification of a HAT domain ligand. We have shown that an intact Utp6 HAT domain is required for binding Utp21. We next set out to identify the specific peptide within Utp21 that binds to the HAT domain. Because known ligands for TPRs are short sequences, we hypothesized that the portion of Utp21 required for binding the Utp6 HAT domain would also be a short sequence. We therefore constructed progressive carboxyl truncated fragments of Utp21 for use in the two-hybrid system (Fig. 7A). We found that a Utp21 fragment ending at residue 279 bound Utp6, but any Utp21 fragment ending at or prior to residue 273 did not. Because it is possible that the truncation at 273 interrupts the binding peptide, we conservatively concluded that the sequence necessary for binding the Utp6 HAT

domain lies between amino acids 267 and 279 (GTSSGDLIF YDLD), as shown in Fig. 7A.

To test whether residues 267 to 279 are sufficient for binding Utp6, we monitored binding by SPR. MBP-Utp6-6HIS, MBP-Utp6-G99E-6HIS, and MBP alone were expressed and purified from *E. coli* (Fig. 7C). We immobilized a synthetic peptide (biotin-GGG-GTSSGDLIF YDLD-CONH₂) on the surface of a NeutraAvidin-coated chip and flowed MBP-Utp6-6HIS or MBP over the chip. MBP-Utp6-6HIS binds to the Utp21 peptide but not to biotin alone (Fig. 7D). Importantly, MBP exhibits no significant binding to the peptide (Fig. 7D). We estimate the dissociation constant for the Utp6-peptide interaction to be approximately 10 μ M (Fig. 7E). A dissociation constant of this magnitude is consistent with that reported for TPR-peptide interactions (10, 45).

Because the two-hybrid results showed that the G99E mutation in the Utp6 HAT domain abrogated binding to Utp21,

we tested the effect of this mutation on binding *in vitro*. MBP-Utp6-G99E-6HIS shows minimal detectable binding to the Utp21 peptide, even at concentrations comparable to those tested for MBP-Utp6-6HIS, in which significant binding was observed (Fig. 7D and E). Thus, the G99E point mutation abrogates interaction with the Utp21 peptide. Collectively, these results show that a short peptide sequence in Utp21 is both necessary and sufficient for binding the Utp6 HAT domain.

DISCUSSION

The SSU processome is a large ribonucleoprotein particle of which most of the members have been identified, but the structure and assembly of this macromolecule remain largely unknown. We have constructed an interaction map for the UtpB subcomplex of the SSU processome and defined further the interaction between Utp6 and Utp21. We have identified the specific peptide within Utp21 that binds to the HAT domain in Utp6, the first known HAT domain-peptide ligand interaction. Additionally, we have shown that a mutation in Utp6 (G99E) that disrupts Utp21 binding, as shown by both two-hybrid and by SPR, also causes a defect in pre-rRNA processing and cell growth, the latter effect being exacerbated by lowered temperature.

We propose that disruption of the Utp6-Utp21 interaction causes a defect in the efficiency of SSU processome assembly that results in an inhibition of ribosome biogenesis. Early studies in *E. coli* have shown that, due to the large amount of energy required for structural rearrangements of the ribosomal intermediate particle, the production rate is dependent on temperature (23). To attest to this, a genome-wide genetic screen for mutations that confer cold sensitivity yielded defects in ribosome assembly (23). Likewise, we have shown that mutations in Utp6 that confer cold sensitivity also produce defects in pre-rRNA processing and slowed growth at lowered temperatures (Fig. 3 and 4). Interestingly, the G99E mutation, which abolishes the interaction between Utp6 and Utp21, does not completely prohibit Utp6 from associating with Mpp10, a non-UtpB subcomplex member of the SSU processome that we use as a surrogate for assembly of the SSU processome (Fig. 5). However, because the immunoprecipitation assay measures the steady-state association of these proteins, this assay would not report the efficiency of assembly. In addition, Utp6 can be recruited into the UtpB subcomplex by its association with Utp18, which is not disrupted by the G99E mutation (Fig. 6). Utp6 may also make additional contacts with other proteins or rRNA. These other contacts may aid in SSU processome assembly. Therefore, disruption of the Utp6-Utp21 interaction likely causes a structural instability that slows SSU processome assembly and renders pre-rRNA processing inefficient.

The UtpB subcomplex proteins were identified based on their copurification in a large-scale study (Table 1) (29), but the architecture and organization of the complex and direct interactions among the proteins remained largely unknown: only the interaction between Utp18 and Utp21 had been identified by a large-scale yeast two-hybrid (26). Here, we have defined six additional interactions via a two-hybrid screen, providing a comprehensive structural map of the subcomplex net-

work (Fig. 6). Though it is a concern that the two-hybrid approach may not accurately reflect direct interactions between yeast proteins, we believe that the interactions we have observed presently are indeed direct. If indirect interactions were to yield a positive result, we would expect each pair tested to be positive because we already know that these six proteins form a subcomplex. However, relatively few interactions are actually observed. Previous use of the two-hybrid system in determining the architecture of a multiprotein complex has indicated that, because the two-hybrid fusion proteins are overexpressed, the endogenous expression of a potential linker protein would not be sufficient to activate expression of the reporter (25).

Curiously, we were not able to determine an essential role for the C-terminal half of Utp6. We identified several serendipitous mutations that truncate the protein shortly C-terminal to the HAT domain, deleting the C-terminal half of the protein, but these truncated proteins support growth more or less normally at the permissive temperature. We therefore concluded that the C-terminal half of the protein is not essential for viability. Additionally, we did not identify a binding partner for this portion of the protein. What is its role? It is likely that many SSU processome proteins bind the pre-rRNA in order to aid in proper pre-rRNA folding, so the C terminus of Utp6 may have an RNA-binding function. Alternatively, it may mediate self-dimerization similar to that found in the C-terminal portion of CstF-77, another HAT-containing protein (3, 30). Though we found via the two-hybrid assay that Utp6 self-associates (Fig. 6), we have not further investigated these possibilities.

Speculations about the structure and function of the HAT domain have been made based on its sequence similarities to the TPR domain. The recent crystal structure of the HAT protein CstF-77 has shown that, as in TPRs, each HAT repeat folds into two alpha helices that pack in an antiparallel manner, a structure that is very similar to that of the TPR domain (3, 30). However, while the TPR domain is found in proteins of various functions, the HAT domain is found only in proteins in RNA processing complexes, leading to the notion that the HAT domain may bind RNA instead of protein (8, 42, 44). We have shown here that the Utp6 HAT domain binds to a short, unstructured peptide in Utp21. This suggests that the restriction of HAT domains to proteins in RNA processing complexes is likely a consequence of their shared evolutionary history rather than because the HAT domains bind RNA.

ACKNOWLEDGMENTS

We thank members of the Regan laboratory for technical advice and helpful conversations. We are grateful to Sander Granneman for suggestions regarding protein purification and to Baserga laboratory members for advice, discussion, technical assistance, and critical reading of the manuscript.

This investigation was supported by National Research Service Award T32 HD07149 from the NIH (E.A.C.), the Arnold and Mabel Beckman Foundation (B.H.L.), a subcontract from GM080515 (L.R.), and NIGMS grant number 52581 (S.J.B.).

REFERENCES

- Amada, N., T. Tezuka, A. Mayeda, K. Araki, N. Takei, K. Todokoro, and H. Nawa. 2003. A novel rat orthologue and homologue for the *Drosophila* crooked neck gene in neural stem cells and their immediate descendants. *J. Biochem.* 133:615–623.
- Ausubel, F. M., R. Brent, R. E. Kingston, D. D. Moore, J. G. Seidman, J. A. Smith, and K. Struhl (ed.). 1995. Short protocols in molecular biology: a

- compendium of methods from current protocols in molecular biology, 3rd ed. Wiley, New York, NY.
3. **Bai, Y., T. C. Auperin, C. Y. Chou, G. G. Chang, J. L. Manley, and L. Tong.** 2007. Crystal structure of murine CstF-77: dimeric association and implications for polyadenylation of mRNA precursors. *Mol. Cell* **25**:863–875.
 4. **Ben-Yehuda, S., I. Dix, C. S. Russell, M. McGarvey, J. D. Beggs, and M. Kupiec.** 2000. Genetic and physical interactions between factors involved in both cell cycle progression and pre-mRNA splicing in *Saccharomyces cerevisiae*. *Genetics* **156**:1503–1517.
 5. **Bernstein, K. A., J. E. Gallagher, B. M. Mitchell, S. Granneman, and S. J. Baserga.** 2004. The small-subunit processome is a ribosome assembly intermediate. *Eukaryot. Cell* **3**:1619–1626.
 6. **Bleichert, F., S. Granneman, Y. N. Osheim, A. L. Beyer, and S. J. Baserga.** 2006. The PINc domain protein Utp24, a putative nuclease, is required for the early cleavage steps in 18S rRNA maturation. *Proc. Natl. Acad. Sci. USA* **103**:9464–9469.
 7. **Carrigan, P. E., L. A. Sikkink, D. F. Smith, and M. Ramirez-Alvarado.** 2006. Domain:domain interactions within Hop, the Hsp70/Hsp90 organizing protein, are required for protein stability and structure. *Protein Sci.* **15**:522–532.
 8. **Chung, S., M. R. McLean, and B. C. Rymond.** 1999. Yeast ortholog of the *Drosophila* crooked neck protein promotes spliceosome assembly through stable U4/U6.U5 snRNP addition. *RNA* **5**:1042–1054.
 9. **Chung, S., Z. Zhou, K. A. Huddleston, D. A. Harrison, R. Reed, T. A. Coleman, and B. C. Rymond.** 2002. Crooked neck is a component of the human spliceosome and implicated in the splicing process. *Biochim. Biophys. Acta* **1576**:287–297.
 10. **Cortajarena, A. L., and L. Regan.** 2006. Ligand binding by TPR domains. *Protein Sci.* **15**:1193–1198.
 11. **D'Andrea, L. D., and L. Regan.** 2003. TPR proteins: the versatile helix. *Trends Biochem. Sci.* **28**:655–662.
 12. **De Raedt, T., H. Brems, C. Lopez-Correa, J. R. Vermeesch, P. Marynen, and E. Legius.** 2004. Genomic organization and evolution of the NF1 microdeletion region. *Genomics* **84**:346–360.
 13. **Dosil, M., and X. R. Bustelo.** 2004. Functional characterization of Pwp2, a WD family protein essential for the assembly of the 90 S pre-ribosomal particle. *J. Biol. Chem.* **279**:37385–37397.
 14. **Dragon, F., J. E. Gallagher, P. A. Compagnone-Post, B. M. Mitchell, K. A. Porwancher, K. A. Wehner, S. Wormsley, R. E. Settlege, J. Shabanowitz, Y. Osheim, A. L. Beyer, D. F. Hunt, and S. J. Baserga.** 2002. A large nucleolar U3 ribonucleoprotein required for 18S ribosomal RNA biogenesis. *Nature* **417**:967–970.
 15. **Dunbar, D. A., S. Wormsley, T. M. Agentis, and S. J. Baserga.** 1997. Mpp10p, a U3 small nucleolar ribonucleoprotein component required for pre-18S rRNA processing in yeast. *Mol. Cell. Biol.* **17**:5803–5812.
 16. **Fatica, A., and D. Tollervey.** 2002. Making ribosomes. *Curr. Opin. Cell Biol.* **14**:313–318.
 17. **Fromont-Racine, M., B. Senger, C. Saveanu, and F. Fasiolo.** 2003. Ribosome assembly in eukaryotes. *Gene* **313**:17–42.
 18. **Gallagher, J. E., and S. J. Baserga.** 2004. Two-hybrid Mpp10p interaction-defective Imp4 proteins are not interaction defective in vivo but do confer specific pre-rRNA processing defects in *Saccharomyces cerevisiae*. *Nucleic Acids Res.* **32**:1404–1413.
 19. **Gallagher, J. E., D. A. Dunbar, S. Granneman, B. M. Mitchell, Y. Osheim, A. L. Beyer, and S. J. Baserga.** 2004. RNA polymerase I transcription and pre-rRNA processing are linked by specific SSU processome components. *Genes Dev.* **18**:2506–2517.
 20. **Goldenberg, D. P.** 1988. Genetic studies of protein stability and mechanisms of folding. *Annu. Rev. Biophys. Chem.* **17**:481–507.
 21. **Grandi, P., V. Rybin, J. Bassler, E. Pefalski, D. Strauss, M. Marzoch, T. Schafer, B. Kuster, H. Tschochner, D. Tollervey, A. C. Gavin, and E. Hurt.** 2002. 90S pre-ribosomes include the 35S pre-rRNA, the U3 snoRNP, and 40S subunit processing factors but predominantly lack 60S synthesis factors. *Mol. Cell* **10**:105–115.
 22. **Granneman, S., and S. J. Baserga.** 2004. Ribosome biogenesis: of knobs and RNA processing. *Exp. Cell Res.* **296**:43–50.
 23. **Guthrie, C., H. Nashimoto, and M. Nomura.** 1969. Structure and function of *E. coli* ribosomes. 8. Cold-sensitive mutants defective in ribosome assembly. *Proc. Natl. Acad. Sci. USA* **63**:384–391.
 24. **Henras, A. K., J. Soudet, M. Gerus, S. Lebaron, M. Caizergues-Ferrer, A. Mougins, and Y. Henry.** 2008. The post-transcriptional steps of eukaryotic ribosome biogenesis. *Cell Mol. Life Sci.* **65**:2334–2354.
 25. **Houser-Scott, F., S. Xiao, C. E. Millikin, J. M. Zengel, L. Lindahl, and D. R. Engelke.** 2002. Interactions among the protein and RNA subunits of *Saccharomyces cerevisiae* nuclear RNase P. *Proc. Natl. Acad. Sci. USA* **99**:2684–2689.
 26. **Ito, T., T. Chiba, R. Ozawa, M. Yoshida, M. Hattori, and Y. Sakaki.** 2001. A comprehensive two-hybrid analysis to explore the yeast protein interactome. *Proc. Natl. Acad. Sci. USA* **98**:4569–4574.
 27. **James, P., J. Halladay, and E. A. Craig.** 1996. Genomic libraries and a host strain designed for highly efficient two-hybrid selection in yeast. *Genetics* **144**:1425–1436.
 28. **Jenne, D. E., S. Tinschert, M. O. Dorschner, H. Hameister, K. Stephens, and H. Kehrer-Sawatzki.** 2003. Complete physical map and gene content of the human NF1 tumor suppressor region in human and mouse. *Genes Chromosomes Cancer* **37**:111–120.
 29. **Krogan, N. J., W. T. Peng, G. Cagney, M. D. Robinson, R. Haw, G. Zhong, X. Guo, X. Zhang, V. Canadien, D. P. Richards, B. K. Beattie, A. Lalev, W. Zhang, A. P. Davierwala, S. Mnaimneh, A. Starostine, A. P. Tikuisis, J. Grigull, N. Datta, J. E. Bray, T. R. Hughes, A. Emili, and J. F. Greenblatt.** 2004. High-definition macromolecular composition of yeast RNA-processing complexes. *Mol. Cell* **13**:225–239.
 30. **Legrand, P., N. Pinaud, L. Minvielle-Sebastia, and S. Fribourg.** 2007. The structure of the CstF-77 homodimer provides insights into CstF assembly. *Nucleic Acids Res.* **35**:4515–4522.
 31. **Liu, S., R. Rauhut, H. P. Vornlocher, and R. Luhrmann.** 2006. The network of protein-protein interactions within the human U4/U6.U5 tri-snRNP. *RNA* **12**:1418–1430.
 32. **Magliery, T. J., and L. Regan.** 2005. Sequence variation in ligand binding sites in proteins. *BMC Bioinformatics* **6**:240.
 33. **Main, E. R., Y. Xiong, M. J. Cocco, L. D'Andrea, and L. Regan.** 2003. Design of stable alpha-helical arrays from an idealized TPR motif. *Structure* **11**:497–508.
 34. **McLean, M. R., and B. C. Rymond.** 1998. Yeast pre-mRNA splicing requires a pair of U1 snRNP-associated tetratricopeptide repeat proteins. *Mol. Cell. Biol.* **18**:353–360.
 35. **Miller, O. L., Jr., and B. R. Beatty.** 1969. Visualization of nucleolar genes. *Science* **164**:955–957.
 36. **Minvielle-Sebastia, L., B. Winsor, N. Bonneaud, and F. Lacroute.** 1991. Mutations in the yeast RNA14 and RNA15 genes result in an abnormal mRNA decay rate; sequence analysis reveals an RNA-binding domain in the RNA15 protein. *Mol. Cell. Biol.* **11**:3075–3087.
 37. **Mougey, E. B., L. K. Pape, and B. Sollner-Webb.** 1993. A U3 small nuclear ribonucleoprotein-requiring processing event in the 5' external transcribed spacer of *Xenopus* precursor rRNA. *Mol. Cell. Biol.* **13**:5990–5998.
 38. **Muhlrad, D., R. Hunter, and R. Parker.** 1992. A rapid method for localized mutagenesis of yeast genes. *Yeast* **8**:79–82.
 39. **Mumberg, D., R. Muller, and M. Funk.** 1995. Yeast vectors for the controlled expression of heterologous proteins in different genetic backgrounds. *Gene* **156**:119–122.
 40. **Osheim, Y. N., S. L. French, K. M. Keck, E. A. Champion, K. Spasov, F. Dragon, S. J. Baserga, and A. L. Beyer.** 2004. Pre-18S ribosomal RNA is structurally compacted into the SSU processome prior to being cleaved from nascent transcripts in *Saccharomyces cerevisiae*. *Mol. Cell* **16**:943–954.
 41. **Perez-Fernandez, J., A. Roman, J. De Las Rivas, X. R. Bustelo, and M. Dosil.** 2007. The 90S pre-ribosome is a multimodular structure that is assembled through a hierarchical mechanism. *Mol. Cell. Biol.* **27**:5414–5429.
 42. **Preker, P. J., and W. Keller.** 1998. The HAT helix, a repetitive motif implicated in RNA processing. *Trends Biochem. Sci.* **23**:15–16.
 43. **Roske, K., M. J. Calcutt, and K. S. Wise.** 2004. The *Mycobacterium fermentans* prophage phiMFV1: genome organization, mobility and variable expression of an encoded surface protein. *Mol. Microbiol.* **52**:1703–1720.
 44. **Sane, A. P., B. Stein, and P. Westhoff.** 2005. The nuclear gene HCF107 encodes a membrane-associated R-TPR (RNA tetratricopeptide repeat)-containing protein involved in expression of the plastidial *psbH* gene in *Arabidopsis*. *Plant J.* **42**:720–730.
 45. **Scheuffer, C., A. Brinker, G. Bourenkov, S. Pegoraro, L. Moroder, H. Bartunik, F. U. Hartl, and I. Moarefi.** 2000. Structure of TPR domain-peptide complexes: critical elements in the assembly of the Hsp70-Hsp90 multichaperone machine. *Cell* **101**:199–210.
 46. **Stanek, D., S. D. Rader, M. Klingauf, and K. M. Neugebauer.** 2003. Targeting of U4/U6 small nuclear RNP assembly factor SART3/p110 to Cajal bodies. *J. Cell Biol.* **160**:505–516.
 47. **Torchet, C., C. Jacq, and S. Hermann-Le Denmat.** 1998. Two mutant forms of the S1/TPR-containing protein Rrp5p affect the 18S rRNA synthesis in *Saccharomyces cerevisiae*. *RNA* **4**:1636–1652.
 48. **Venturin, M., P. Guarnieri, F. Natacci, M. Stabile, R. Tenconi, M. Clementi, C. Hernandez, P. Thompson, M. Upadhyaya, L. Larizza, and P. Riva.** 2004. Mental retardation and cardiovascular malformations in NF1 microdeletion patients point to candidate genes in 17q11.2. *J. Med. Genet.* **41**:35–41.
 49. **Verschoor, A., J. R. Warner, S. Srivastava, R. A. Grassucci, and J. Frank.** 1998. Three-dimensional structure of the yeast ribosome. *Nucleic Acids Res.* **26**:655–661.
 50. **Vincent, K., Q. Wang, S. Jay, K. Hobbs, and B. C. Rymond.** 2003. Genetic interactions with CLF1 identify additional pre-mRNA splicing factors and a link between activators of yeast vesicular transport and splicing. *Genetics* **164**:895–907.
 51. **Warner, J. R.** 1999. The economics of ribosome biosynthesis in yeast. *Trends Biochem. Sci.* **24**:437–440.
 52. **Wehner, K. A., J. E. Gallagher, and S. J. Baserga.** 2002. Components of an interdependent unit within the SSU processome regulate and mediate its activity. *Mol. Cell. Biol.* **22**:7258–7267.
 53. **Zhang, K., D. Smouse, and N. Perrimon.** 1991. The crooked neck gene of *Drosophila* contains a motif found in a family of yeast cell cycle genes. *Genes Dev.* **5**:1080–1091.